



Secondary esophageal adenocarcinoma of pulmonary origin: a case description of imaging findings

Huaiyu Zhang^{1^}, Lirong Zhang², Yuangang Qiao¹

¹Department of Radiology, The 8th Medical Center of Chinese PLA General Hospital, Beijing, China; ²Department of Radiology, Beijing Tongren Hospital, Capital Medical University, Beijing, China

Correspondence to: Yuangang Qiao. Department of Radiology, The 8th Medical Center of Chinese PLA General Hospital, Beijing 100091, China. Email: qiaoyg1@163.com.

Submitted Jan 26, 2022. Accepted for publication Jun 01, 2022.

doi: 10.21037/qims-22-84

View this article at: <https://dx.doi.org/10.21037/qims-22-84>

Introduction

Esophageal cancer (EC) is the sixth most common cancer globally (1). Esophageal squamous cell carcinoma, the dominant subtype of EC, is the fourth leading cause of cancer-related deaths in China (2). Secondary esophageal adenocarcinoma is clinically rare. It generally refers to a neoplasm that occurs when direct invasion of primary malignant tumors of tissues and organs outside the esophagus or the passage of tumor cells through lymph and blood causes destruction and canceration of esophageal tissue structure (3). To date, only a few reports have examined imaging manifestations of secondary esophageal neoplasms. Here, we present a case of secondary pulmonary esophageal adenocarcinoma and describe its findings according to computed tomography (CT) pre-radiotherapy and gastrointestinal radiography and CT after radiotherapy.

Case presentation

A 72-year-old man had experienced chest and back pain for more than 3 months and a choking sensation when eating for more than 2 months without cough, sputum, chest tightness, or chest pain. Gastroscopy revealed a cauliflower-like mass 30 cm from the incisors covered with moss, with a narrow lumen and a lesion extending approximately 4 cm downwards. Immunohistochemistry showed TTF-1 (+), Napsin A (+), CK7 (+), CK20 (-),

CK8 (+), CK18 (+), CDX2 (+), Villin (-), P40 (-), CK5/6 (-), HER-2 (-), CD56 (-), CgA (-), Syn (-), and Ki-67 (80%). The diagnosis was adenocarcinoma, consistent with a pulmonary origin. Genetic testing suggested *KRAS* (Kirsten rat sarcoma viral oncogene homologue) mutation. Bronchoscopy showed grayish-white tissue with a diameter of 0.2 cm in the posterior bronchial wall at the beginning of the left bronchus. Immunohistochemistry showed TTF-1 (+), Napsin A (+), CK5/6 (-), P40 (-), CK7 (+), and Syn (-), consistent with a diagnosis of adenocarcinoma of the lung. Immunohistochemistry of mediastinal lymph nodes showed TTF-1 (+), Napsin A (+), and CK7 (+), consistent with a diagnosis of a metastatic lymph node from pulmonary adenocarcinoma. Combined with the clinical data and positron emission tomography (PET)-CT (*Figures 1,2*), the tumor tumor-node-metastasis (TNM) stage was T4N2M1b based on the eighth edition of the American Joint Committee on Cancer staging system (4). The patient returned to the 8th Medical Center of Chinese PLA General Hospital for further treatment, and received radiotherapy. The prescribed dose was 40 Gy, administered at a daily 2 Gy/fraction, 5 days/week over 4 weeks (20 fractions). After the 19th dose of radiotherapy, the patient developed an esophageal-respiratory fistula and declined further treatment.

The pre-radiotherapy chest CT showed uneven circumferential thickening of the wall of the lower esophagus and mass formation (*Figure 3A*). Contrast-enhanced

[^] ORCID: 0000-0002-5561-2210.

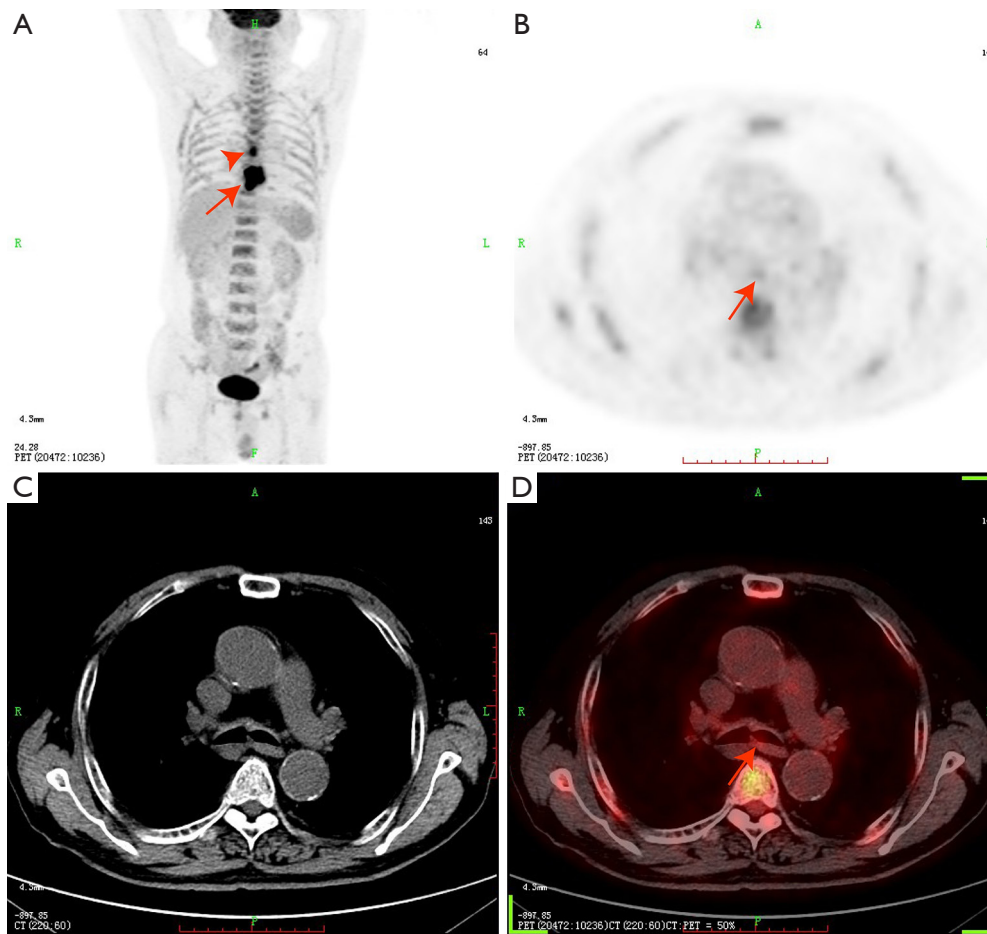


Figure 1 A primary lesion of the left main bronchus, a secondary lesion of the esophagus and a metastatic lymph node in the mediastinum. (A) The metastatic lymph node in the mediastinum and esophageal lesion are displayed in the maximum intensity projection image (red arrowhead and arrow). (B) PET image displayed the primary lesion (red arrow) at the beginning of the left bronchus. (C) No positive findings were found on axial CT. (D) PET/CT image demonstrated the primary lesion (red arrow) at the beginning of the left bronchus increased ^{18}F -FDG uptake. PET, positron emission tomography; CT, computed tomography; ^{18}F -FDG; ^{18}F -fluorodeoxyglucose.

CT showed that the tumor had dramatic progressive enhancement in the venous and delayed phases (*Figure 3B-3D*). The enhancement scan also identified several hypointense lesions and enlarged lymph nodes (*Figure 3E,3F*). Before radiotherapy, the PET-CT showed increased ^{18}F -fluorodeoxyglucose (^{18}F -FDG) uptake in the primary lesion of the posterior wall of the bronchus at the beginning of the left bronchus, esophageal lesions, and metastatic lymph node in the mediastinum (*Figures 1,2*).

During radiotherapy, the patient developed hyperthermia, and post-radiotherapy complications were clinically suspected. Upper gastrointestinal imaging and chest CT revealed an esophageal-respiratory fistula (*Figure 4*). Gastrointestinal images showed the formation

of esophageal sinuses and paramediastinal sinuses (*Figure 4A,4B*). A line-shaped shadow in the lower right lung supported our suspicion that an esophageal-respiratory fistula had formed (*Figure 4C*). Therefore, a chest CT examination was subsequently performed. During the CT, the contrast medium entered the bronchi of the lower lobe of the right lung, confirming the presence of an esophageal-respiratory fistula (*Figure 4D-4F*).

All procedures performed in this study were in accordance with the ethical standards of the institutional and national research committee(s) and with the Helsinki Declaration (as revised in 2013). Written informed consent was provided by the patient for publication of this case report and accompanying images. A copy of the written

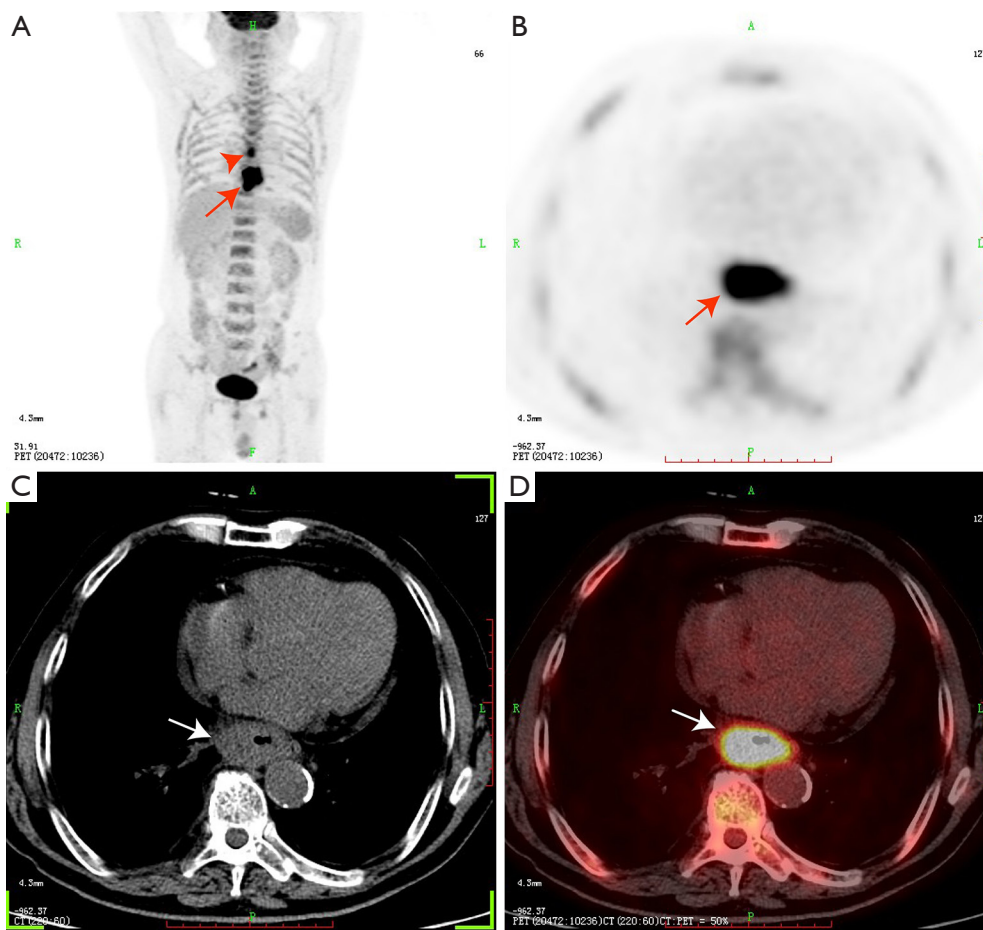


Figure 2 Thickening of the esophageal duct wall. Abnormal ^{18}F -FDG uptake in the esophageal lesion and the metastatic lymph node in the mediastinum. (A,B) The maximum density projection and axial PET image. (C,D) The axial CT and PET/CT image. PET and PET/CT images showed increased ^{18}F -FDG uptake in esophageal lesion (arrows in A, B and D). The mediastinal metastatic lymph node increased ^{18}F -FDG uptake (A, red arrowhead). In addition, axial CT of the mediastinal window showed uneven thickening of the esophageal wall (C, arrow). PET, positron emission tomography; CT, computed tomography; ^{18}F -FDG; ^{18}F -fluorodeoxyglucose.

consent is available for review by the editorial office of this journal.

Discussion

Secondary adenocarcinoma of the esophagus, including secondary invasive carcinoma and secondary metastatic carcinoma, occurs when a primary malignant tumor of any tissue or organ outside the esophagus causes structural destruction and carcinogenesis of the esophagus through direct infiltration or via infiltration of the lymphatic or blood route (3). Existing literature shows that the primary malignancy of secondary EC can arise from the thyroid, breast, lung, liver, kidney, prostate, skin, kidney, bladder,

rectum, pancreas, thyroid, liver, and endometrium (3,5-11). However, detailed studies of imaging features are scarce, and there are no detailed reports of CT-enhanced manifestations. In our current case, the patient underwent CT enhancement before treatment. He had mild enhancement of the solid part of the tumor in the arterial phase after enhancement, and progressive enhancement in the venous and extended phases with marked enhancement. Unlike squamous carcinoma of the esophagus, which commonly intensifies in a typical malignant manner, the patient's tumor showed a reduced degree of intensification during the delayed period.

The imaging presentation of secondary esophageal adenocarcinoma may be related to its mode of metastasis.

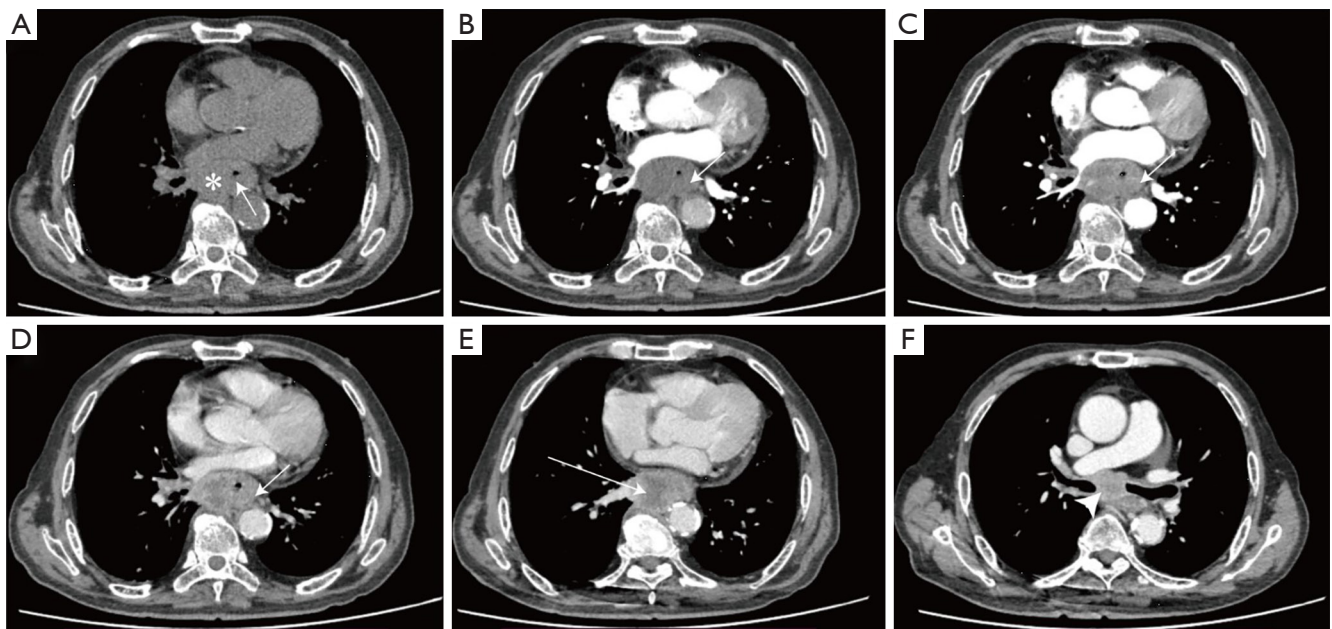


Figure 3 Plain and enhanced CT of the chest. (A) Pre-radiotherapy non-enhanced chest CT shows uneven circumferential thickening of the wall of the lower esophagus (stars) with isodensity (39 HU) and mass formation (white arrow). (B) Mild enhancement (45 HU) of the esophageal wall in the arterial phase (white arrow). (C) The esophageal wall still has increased enhancement (55 HU) in the venous phase (white arrow). (D) Significant strengthening (87 HU) of the esophageal wall during the delayed period (white arrow). (E) Localized hypointense area within the tumor after enhancement suggests possible tumor necrosis (white arrow). (F) Axial enhanced CT show enlarged lymph nodes with enhancement (white arrowhead). CT, computed tomography; HU, Hounsfield units.

Tumor metastases can occur through direct invasion or by hematologic or lymphatic routes. Direct esophageal extension of an adjacent tumor usually manifests as a lateral bulge in the esophageal wall. The CT images will show that the mass in the lung compresses the esophagus and the esophageal lumen is narrow. Metastases from the hematologic and lymphatic routes of the esophagus often present a diagnostic challenge, usually in the form of esophageal strictures that are short in extent and may mimic the primary tumor, presenting as a circumferential thickening of the esophageal wall (3).

Secondary esophageal adenocarcinoma can be treated by radiotherapy, but physicians must remain aware of post-radiation complications such as esophageal-respiratory fistula. Upper gastrointestinal tract radiography and a CT scan immediately after radiotherapy can clarify the occurrence of this complication. Our patient had a sudden onset of fever during radiotherapy; after ruling out other infections, these two tests provided diagnostic assistance. Gastrointestinal imaging allows dynamic visualization of the flow of contrast, rapid detection of the fistula, and clear

visualization of the flow of contrast through the esophageal fistula and through the sinus tract to the paramediastinal sinus cavity and the local bronchi in the lower lobe of the right lung (*Figure 4A-4C*) (12). However, it gastrointestinal imaging requires precision positioning, which CT can complement (13). A CT examination can identify the entrance and exit of the sinus tract and the location of the bronchus into which the contrast medium flows (*Figure 4D-4F*). In cases of suspected esophageal-respiratory fistula formation, the contrast agent of choice for gastrointestinal imaging should be an iodine agent, such as iohexol, rather than barium, because barium can lead to persistent pneumonia as a result of foreign body deposits.

When imaging reveals the presence of a primary lesion in the lung, diagnosing secondary adenocarcinoma of pulmonary origin in the esophagus is relatively easy. However, when the lung tumor is hidden, or there is external pressure from lesions, a secondary malignant tumor is difficult to distinguish from primary EC. In such circumstances, the diagnosis is difficult, and it is easy to make a misdiagnosis.

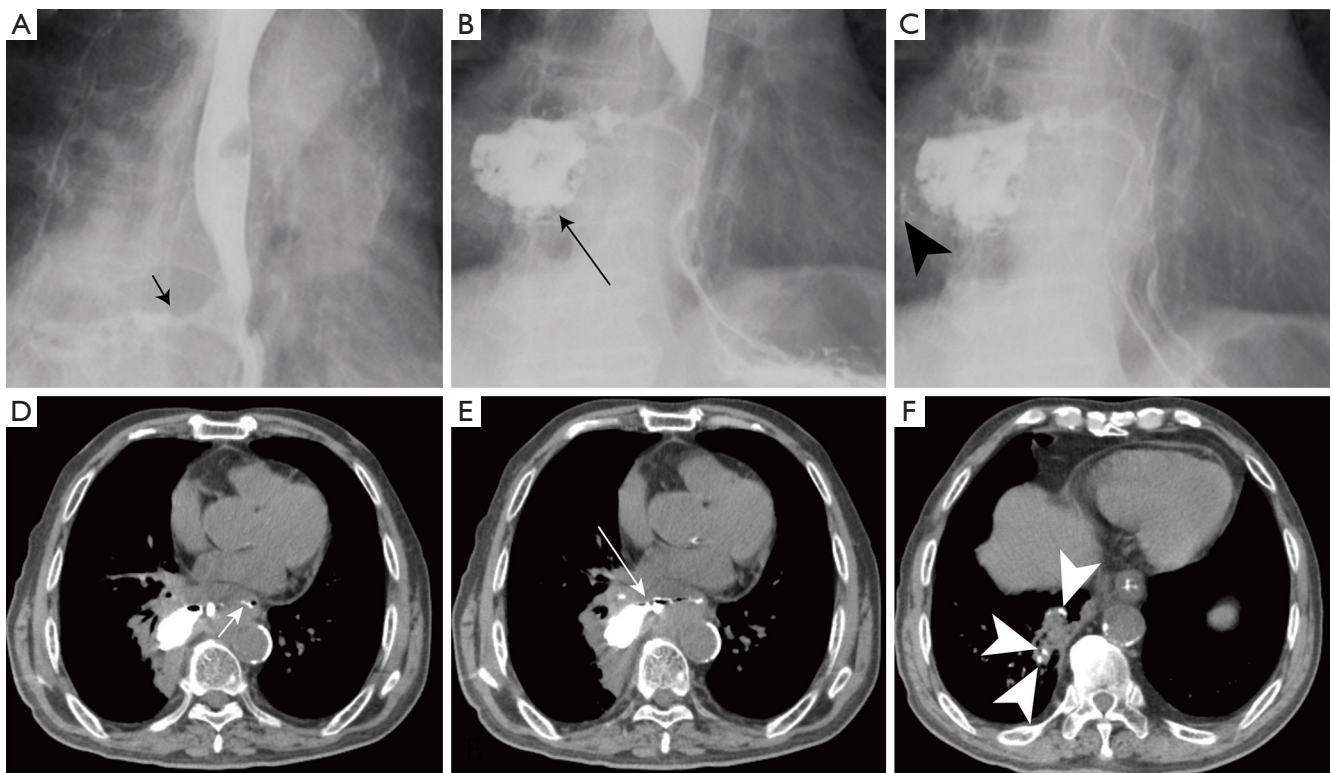


Figure 4 CT and upper gastrointestinal imaging after radiotherapy. (A) Right anterior oblique X-ray shows esophageal sinus tract formation (short black arrow). (B) Mediastinal paranasal sinus cavity is noted in the left anterior oblique image (long black arrow). (C) Radiograph of left anterior oblique indicates a flow of contrast medium into the bronchi of the lower lobe of the right lung (black arrowhead). (D) Axial CT demonstrates the entrance to the esophageal sinus tract (short white arrow). (E) Sinus tract exit is pointed out (long white arrow). (F) The flow of contrast medium into the bronchi of the lower lobe of the right lung is clear on the CT image (white arrowhead). CT, computed tomography.

Radiological examination is extremely helpful in detecting secondary adenocarcinoma of pulmonary origin in the esophagus. Even if the patient has undergone endoscopy, gastrointestinal tract radiography imaging and plain or enhanced CT examination are still necessary to reduce misdiagnosis and missed diagnosis, especially when the tumor enhances in a progressive manner. Vigilance for secondary adenocarcinoma of the esophagus should be increased.

Acknowledgments

Funding: None.

Footnote

Conflicts of Interest: All authors have completed the ICMJE

uniform disclosure form (available at <https://qims.amegroups.com/article/view/10.21037/qims-22-84/coif>). The authors have no conflicts of interest to declare.

Ethical Statement: The authors are accountable for all aspects of the work in ensuring that questions related to the accuracy or integrity of any part of the work are appropriately investigated and resolved. All procedures performed in this study were in accordance with the ethical standards of the institutional and/or national research committee(s) and with the Helsinki Declaration (as revised in 2013). Written informed consent was provided by the patient for publication of this case report and accompanying images. A copy of the written consent is available for review by the editorial office of this journal.

Open Access Statement: This is an Open Access article

distributed in accordance with the Creative Commons Attribution-NonCommercial-NoDerivs 4.0 International License (CC BY-NC-ND 4.0), which permits the non-commercial replication and distribution of the article with the strict proviso that no changes or edits are made and the original work is properly cited (including links to both the formal publication through the relevant DOI and the license). See: <https://creativecommons.org/licenses/by-nc-nd/4.0/>.

References

1. Yang H, Zhang Q, Xu M, Wang L, Chen X, Feng Y, Li Y, Zhang X, Cui W, Jia X. CCL2-CCR2 axis recruits tumor associated macrophages to induce immune evasion through PD-1 signaling in esophageal carcinogenesis. *Mol Cancer* 2020;19:41.
2. Liu Q, Cui X, Yu X, Bian BS, Qian F, Hu XG, Ji CD, Yang L, Ren Y, Cui W, Zhang X, Zhang P, Wang JM, Cui YH, Bian XW. Cripto-1 acts as a functional marker of cancer stem-like cells and predicts prognosis of the patients in esophageal squamous cell carcinoma. *Mol Cancer* 2017;16:81.
3. Agha FP. Secondary neoplasms of the esophagus. *Gastrointest Radiol* 1987;12:187-93.
4. Detterbeck FC, Boffa DJ, Kim AW, Tanoue LT. The Eighth Edition Lung Cancer Stage Classification. *Chest* 2017;151:193-203.
5. Anderson MF, Harell GS. Secondary esophageal tumors. *AJR Am J Roentgenol* 1980;135:1243-6.
6. Cabezas-Camarero S, Puente J, Manzano A, Corona JA, González-Larriba JL, Bernal-Becerra I, Sotelo M, Díaz-Rubio E. Renal cell cancer metastases to esophagus and stomach successfully treated with radiotherapy and pazopanib. *Anticancer Drugs* 2015;26:112-6.
7. Cho A, Ryu M, Yoshinaga Y, Ishikawa Y, Miyazawa Y, Okazumi S, Ochiai T. Hepatocellular carcinoma with unusual metastasis to the esophagus. *Hepatogastroenterology* 2003;50:1143-5.
8. Haney JC, D'Amico TA. Transhiatal esophagogastrectomy for an isolated ovarian cancer metastasis to the esophagus. *J Thorac Cardiovasc Surg* 2004;127:1835-6.
9. Kobayashi M, Itabashi H, Ikeda T, Yamazaki N, Kaji T, Takagane A. Simultaneous occurrence of distant metastases to the small intestine and the thoracic esophagus from anaplastic thyroid carcinoma: a case report. *Surg Case Rep* 2015;1:63.
10. Liu A, Feng Y, Chen B, Li L, Wu D, Qian J, Yang A. A case report of metastatic breast cancer initially presenting with esophageal dysphagia. *Medicine (Baltimore)* 2018;97:e13184.
11. Wang CY, Xu G, Gao C, Wang D. Esophageal metastases from primary lung cancer: a case report. *J Med Case Rep* 2021;15:265.
12. Kim HS, Khemasuwan D, Diaz-Mendoza J, Mehta AC. Management of tracheo-oesophageal fistula in adults. *Eur Respir Rev* 2020;29:200094.
13. Shin JH, Kim JH, Song HY. Interventional management of esophagorespiratory fistula. *Korean J Radiol* 2010;11:133-40.

Cite this article as: Zhang H, Zhang L, Qiao Y. Secondary esophageal adenocarcinoma of pulmonary origin: a case description of imaging findings. *Quant Imaging Med Surg* 2022;12(8):4331-4336. doi: 10.21037/qims-22-84